Nonlinear Dynamical Model of a Soft Viscoelastic Dielectric Elastomer

Junshi Zhang,[1,2] Hualing Chen,[1,3,*] and Dichen Li[1,2]

[1]School of Mechanical Engineering, Xi'an Jiaotong University, Xi'an 710049, China
[2]State Key Laboratory for Manufacturing Systems Engineering, Xi'an Jiaotong University, Xi'an 710054, China
[3]State Key Laboratory for Strength and Vibration of Mechanical Structures, Xi'an Jiaotong University, Xi'an 710049, China

(Received 12 June 2017; revised manuscript received 3 September 2017; published 14 December 2017)

Actuated by alternating stimulation, dielectric elastomers (DEs) show a behavior of complicated nonlinear vibration, implying a potential application as dynamic electromechanical actuators. As is well known, for a vibrational system, including the DE system, the dynamic properties are significantly affected by the geometrical sizes. In this article, a nonlinear dynamical model is deduced to investigate the geometrical effects on dynamic properties of viscoelastic DEs. The DEs with square and arbitrary rectangular geometries are considered, respectively. Besides, the effects of tensile forces on dynamic performances of rectangular DEs with comparably small and large geometrical sizes are explored. Phase paths and Poincaré maps are utilized to detect the periodicity of the nonlinear vibrations of DEs. The resonance characteristics of DEs incorporating geometrical effects are also investigated. The results indicate that the dynamic properties of DEs, including deformation response, vibrational periodicity, and resonance, are tuned when the geometrical sizes vary.

DOI: 10.1103/PhysRevApplied.8.064016

I. INTRODUCTION

As the soft electroactive polymers, dielectric elastomers (DEs) can generate a large deformation under the external stimuli [1–6]. With a combination of mechanical forces and an applied voltage, the induced maximum areal strain can be up to 1692% [7], implying a significant potential application as soft actuators and robots. The reported typical DE actuators include spring rolls [8], balloons [9], tunable lenses [10], flying wings [11], electric fish [12], loudspeakers [13], and energy generators [14].

During DE's actuation, various deformation modes can be induced by different voltage signals [15]. A dc voltage induces a static or quasistatic deformation, and the DEs obtain an invariable deformation eventually. During the past decade, nonlinear modeling and stability analyses of DEs under static deformation have been well investigated and documented in various forms [16–18]. However, when DEs are performed as dynamic electromechanical actuators, such as flying wings [11], electric fish [12], loudspeakers [13], pumps [19], and acoustic absorbers [20], the ac voltage is required. Under such actuations, the inertial effect plays a decisive role in determining DEs' performance, which should be inevitably included.

Recently, with consideration of different configurations, various researchers carried out the nonlinear dynamical modeling of DEs. The two fundamental approaches to establish dynamics governing equations are the method of virtual work [21,22] and the Euler-Lagrange equation [23,24]. However, the geometrical effects on the dynamic properties of DEs are totally ignored in the reported literature [21–28]. Besides, in previous modeling work, many researchers considered only the inertial force in the in-plane directions, while neglecting the inertial force in the thickness direction. DE membranes are generally in a specific thickness, when the DE membranes are in a large in-plane size, the inertial effect in the thickness may be very weak; however, when the in-plane size of DEs is small, the inertial effect in the thickness direction will become very obvious. That is, the combined effects of the geometrical sizes and the inertial forces in three principal directions are very important in practical applications of DE actuators. Furthermore, the negative works done by the viscous damping in three principal directions are basically ignored by many researchers. As we know, for a vibrational system, the dynamic properties, such as resonant frequency, amplitude, and periodicity, are strongly affected by the geometrical sizes. However, investigations on such opening issues have not yet been explored.

Furthermore, the majority of the workhorse DE materials are popularly the electroactive macromolecular polymers, which exhibit different levels of viscoelasticity [28–33]. Viscoelasticity causes the deformation to have a significant time dependence, dissipates the mechanical energy, and suppresses the amplitude of vibration. Also, a strong viscoelasticity may induce the drifting behavior of the mean stretch of DEs during vibration [32,33], which

*Corresponding author.
hlchen@mail.xjtu.edu.cn

enhances the difficulty in practical applications. Recently, Gu *et al.* [33] developed a theoretical and experimental study on the viscoelastic electromechanical behaviors of DEs, indicative of the obvious phenomena of drift and hysteresis. Therefore, the viscoelastic effects should be involved in developing the DEs' dynamical model.

In this paper, by utilizing the method of virtual work, we deduce a dynamical model of viscoelastic DEs by considering the geometrical effects. Based on the dynamical model, the dynamic properties of DEs are explored. Through the phase paths and Poincaré maps, we also analyze the vibrational periodicity evolution of DEs when the geometry varies.

II. NONLINEAR DYNAMICAL MODEL OF VISCOELASTIC DES

As illustrated in Fig. 1(a), a DE membrane of initial length L_1, width L_2, and thickness H in the reference state, is employed to deduce the dynamical model. The compliant electrodes are coated on both surfaces of the DEs for electroactuation. Subject to the tensile forces P_1 and P_2, and a high voltage ϕ, the DE deforms to the actuated state. We set the three principal stretches as follows: the stretch in length direction is λ_1, the stretch in width direction is λ_2, and the stretch in thickness direction is λ_h. Hence, the DE in the actuated state deforms to the length $L_1\lambda_1$, width $L_2\lambda_2$, and thickness $H\lambda_h$, as shown in Fig. 1(b). Since the Poisson ratio of DEs is approximately 0.5, it is generally regarded that DE membranes are incompressible [34], that is, $\lambda_1\lambda_2\lambda_h = 1$. Therefore, the stretch in thickness direction is obtained as $\lambda_h = \lambda_1^{-1}\lambda_2^{-1}$.

As mentioned previously, the majority of the widely used DE materials exhibit different levels of viscoelasticity. To describe the viscoelastic behavior of DEs, Wissler and Mazza [35] first proposed the Prony series model. Subsequently, based on the theory of rheology, Foo *et al.* [36] and Hong [37] reported that the DEs can be approximately represented by a rheological model that includes two parallel units, i.e., the standard linear solid (SLS) model. Afterwards, Khan *et al.* [38] established the generalized Maxwell viscoelastic model by paralleling

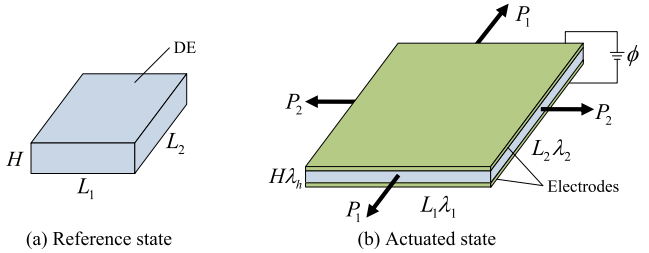

FIG. 1. (a) In the reference state, a DE membrane of initial length L_1, width L_2, and thickness H. (b) In the actuated state, subject to the tensile forces P_1 and P_2, and a high voltage ϕ, the DE deforms, with three principal stretches λ_1, λ_2, and λ_h.

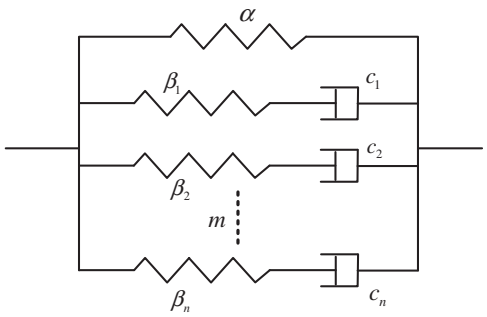

FIG. 2. The Wiechert model: one unit consists of a reversible spring α, and the other unit consists of a group of Maxwell arms which include the springs β_m and the series-wound viscous dampings c_m $(m = 1, 2, 3, \ldots, n)$.

three units of the Maxwell model. Subsequently, to capture both the initial jumping deformation and the following slow creeping of DEs under step stimulations, Zhang *et al.* [39] proposed the Kelvin-Voigt-Maxwell model by parallel connecting the Kelvin-Voigt model and Maxwell model. In this paper, to be more accurate, we adopt the Wiechert model [33,40,41] to describe the viscoelasticity of DEs, as sketched in Fig. 2. In the Wiechert model, one unit consists of a reversible spring α, and the other unit consists of a group of Maxwell arms which includes the springs β_m and the series-wound viscous dampings c_m $(m = 1, 2, 3, \ldots n)$. By employing the Wiechert model, the principal stretch λ_i $(i = 1, 2, h)$ is regarded as the stretch of both units, which is also the stretch of spring α. For an arbitrary Maxwell arm, the stretch of spring β_m is described by λ_{im}^e and is determined by a well-established multiplication rule [33,36,37,39,42] as $\lambda_{im}^e = \lambda_i/\xi_{im}(i = 1, 2, h; m = 1, 2, 3, \ldots, n)$, in which ξ_{im} represents the principal stretches in the viscous damping.

Thus, with the employment of the Gent model [43], the free-energy density function of DEs is obtained as

$$W = -\frac{\mu^\alpha J^\alpha}{2}\log\left(1 - \frac{\lambda_1^2 + \lambda_2^2 + \lambda_1^{-2}\lambda_2^{-2} - 3}{J^\alpha}\right) - \sum_{m=1}^{n}\frac{\mu_m^\beta J_m^\beta}{2}\log\left(1 - \frac{\lambda_1^2\xi_{1m}^{-2} + \lambda_2^2\xi_{2m}^{-2} + \lambda_1^{-2}\lambda_2^{-2}\xi_{1m}^2\xi_{2m}^2 - 3}{J_m^\beta}\right) + \frac{D^2}{2\varepsilon}, \quad (1)$$

where ε is the permittivity, μ^α and μ_m^β are the shear moduli of spring α and springs β_m, J^α, and J_m^β are the material constants related to the limiting stretches of the springs, D is the electric displacement, and is defined as $D = Q/(L_1L_2\lambda_1\lambda_2)$, where Q is the charge on DE surfaces. The free-energy density is extensively utilized to deduce the dynamical model of DEs, and a good agreement between theoretical modeling and experimental measures has been demonstrated [44].

During the actuation, the viscous damping does negative work and dissipates energy. The work done by the viscous damping in three principal directions can be calculated as [39] $(-c_m L_i^2/2)(d\xi_{im}/dt)\delta\xi_{im}(i=1,2)$, and $(-c_m H^2/2)(d\xi_{hm}/dt)\delta\xi_{hm}$, where t denotes the time, and c_m is the viscous damping. On the other hand, when the ac voltage is applied, the DEs vibrate nonlinearly, and the inertial forces should be involved. As reported previously, the work done by the inertial forces in three principal directions can be calculated as [22] $(-\rho L_1 L_2 L_3 L_i^2/3)(d^2\lambda_i/dt^2)\delta\lambda_i(i=1,2)$, and $(-\rho H^3 L_1 L_2/3)(d^2\lambda_h/dt^2)\delta\lambda_h$, in which ρ is the density of DEs. For a viscoelastic DE system, it can be derived that the variation of the free-energy of DEs is equal to the work done jointly by the voltage, the tensile forces, the viscous dampings, and the inertial forces, that is,

$$L_1 L_2 H\delta W = \phi\delta Q + \sum_{i=1}^{2} P_i L_i \delta\lambda_i - \sum_{i=1}^{2}\left(\sum_{m=1}^{n}\frac{c_m L_i^2}{2}\frac{d\xi_{im}}{dt}\delta\xi_{im}\right) - \sum_{m=1}^{n}\frac{c_m H^2}{2}\frac{d\xi_{hm}}{dt}\delta\xi_{hm} - \sum_{i=1}^{2}\left(\frac{\rho L_1 L_2 H L_i^2}{3}\frac{d^2\lambda_i}{dt^2}\delta\lambda_i\right) - \frac{\rho L_1 L_2 H^3}{3}\frac{d^2\lambda_h}{dt^2}\delta\lambda_h. \tag{2}$$

According to the incompressibility of DEs, it can be implied that the inertial force and the viscous damping in the thickness direction can be expressed as

$$\frac{d^2\lambda_h}{dt^2} = -\lambda_1^{-2}\lambda_2^{-1}\frac{d^2\lambda_1}{dt^2} - \lambda_1^{-1}\lambda_2^{-2}\frac{d^2\lambda_2}{dt^2} + 2\lambda_1^{-3}\lambda_2^{-1}\left(\frac{d\lambda_1}{dt}\right)^2 + 2\lambda_1^{-1}\lambda_2^{-3}\left(\frac{d\lambda_2}{dt}\right)^2 + 2\lambda_1^{-2}\lambda_2^{-2}\frac{d\lambda_1}{dt}\frac{d\lambda_2}{dt}, \tag{3}$$

and

$$\frac{d\xi_{hm}}{dt} = -\xi_{1m}^{-2}\xi_{2m}^{-1}\frac{d\xi_{1m}}{dt} - \xi_{1m}^{-1}\xi_{2m}^{-2}\frac{d\xi_{2m}}{dt}. \tag{4}$$

Meanwhile, the variations of λ_h and ξ_h in the thickness direction are obtained as

$$\delta\lambda_h = -\lambda_1^{-2}\lambda_2^{-1}\delta\lambda_1 - \lambda_1^{-1}\lambda_2^{-2}\delta\lambda_2 \tag{5}$$

and

$$\delta\xi_{hm} = -\xi_{1m}^{-2}\xi_{2m}^{-1}\delta\xi_{1m} - \xi_{1m}^{-1}\xi_{2m}^{-2}\delta\xi_{2m}. \tag{6}$$

On the basis of Eqs. (2)–(6), replacing the charge Q with the electric displacement D yields

$$\frac{\partial W}{\partial\lambda_i} = \frac{P_i}{L_j H} + \frac{\phi D}{H}\lambda_j - \frac{\rho L_i^2}{3}\frac{d^2\lambda_i}{dt^2} + \frac{\rho H^2}{3}\lambda_i^{-2}\lambda_j^{-1}\left[-\lambda_i^{-2}\lambda_j^{-1}\frac{d^2\lambda_i}{dt^2} - \lambda_i^{-1}\lambda_j^{-2}\frac{d^2\lambda_j}{dt^2} + 2\lambda_i^{-3}\lambda_j^{-1}\left(\frac{d\lambda_i}{dt}\right)^2 + 2\lambda_i^{-1}\lambda_j^{-3}\left(\frac{d\lambda_j}{dt}\right)^2 + 2\lambda_i^{-2}\lambda_j^{-2}\frac{d\lambda_i}{dt}\frac{d\lambda_j}{dt}\right], \tag{7a}$$

$$\frac{\partial W}{\partial\xi_{im}} = -\frac{c_m L_i}{2L_j H}\frac{d\xi_{im}}{dt} - \frac{c_m H}{2L_i L_j}\xi_{im}^{-2}\xi_{jm}^{-1}\left(\xi_{im}^{-2}\xi_{jm}^{-1}\frac{d\xi_{im}}{dt} + \xi_{im}^{-1}\xi_{jm}^{-2}\frac{d\xi_{jm}}{dt}\right), \tag{7b}$$

$$\frac{\partial W}{\partial D} = \frac{\phi}{H}\lambda_i\lambda_j. \tag{7c}$$

When $i=1$ and $j=2$, Eqs. (7a) and (7b) describe the variations of deformation in length direction; and when $i=2$ and $j=1$, Eqs. (7a) and (7b) describe the variations of deformation in width direction. The indices i and j and their values also apply to the following formula derivations.

According to Eq. (1), we obtain

$$\frac{\partial W}{\partial \lambda_i}=\frac{\mu^{\alpha}(\lambda_i-\lambda_i^{-3}\lambda_j^{-2})}{1-(\lambda_i^2+\lambda_j^2+\lambda_i^{-2}\lambda_j^{-2}-3)/J^{\alpha}}+\sum_{m=1}^{n}\frac{\mu_m^{\beta}(\lambda_i\xi_{im}^{-2}-\lambda_i^{-3}\lambda_j^{-2}\xi_{im}^2\xi_{jm}^2)}{1-(\lambda_i^2\xi_{im}^{-2}+\lambda_j^2\xi_{jm}^{-2}+\lambda_i^{-2}\lambda_j^{-2}\xi_{im}^2\xi_{jm}^2-3)/J_m^{\beta}}, \tag{8a}$$

$$\frac{\partial W}{\partial \xi_{im}}=-\frac{\mu_m^{\beta}(\lambda_i^2\xi_{im}^{-3}-\lambda_i^{-2}\lambda_j^{-2}\xi_{im}\xi_{jm}^2)}{1-(\lambda_i^2\xi_{im}^{-2}+\lambda_j^2\xi_{jm}^{-2}+\lambda_i^{-2}\lambda_j^{-2}\xi_{im}^2\xi_{jm}^2-3)/J_m^{\beta}}, \tag{8b}$$

$$\frac{\partial W}{\partial D}=\frac{D}{\varepsilon}. \tag{8c}$$

Combing Eqs. (7) and (8), and eliminating the electric displacement D, we obtain

$$\left(\frac{\rho L_i^2}{3\mu^{\alpha}}+\frac{\rho H^2}{3\mu^{\alpha}}\lambda_i^{-4}\lambda_j^{-2}\right)\frac{d^2\lambda_i}{dt^2}+\frac{\rho H^2}{3\mu^{\alpha}}\lambda_i^{-3}\lambda_j^{-3}\frac{d^2\lambda_j}{dt^2}-\frac{2\rho H^2}{3\mu^{\alpha}}\lambda_i^{-2}\lambda_j^{-1}\left[\lambda_i^{-3}\lambda_j^{-1}\left(\frac{d\lambda_i}{dt}\right)^2+\lambda_i^{-1}\lambda_j^{-3}\left(\frac{d\lambda_j}{dt}\right)^2+\lambda_i^{-2}\lambda_j^{-2}\frac{d\lambda_i}{dt}\frac{d\lambda_j}{dt}\right]$$
$$+\frac{\lambda_i-\lambda_i^{-3}\lambda_j^{-2}}{1-(\lambda_i^2+\lambda_j^2+\lambda_i^{-2}\lambda_j^{-2}-3)/J^{\alpha}}+\sum_{m=1}^{n}\frac{\mu_m^{\beta}}{\mu^{\alpha}}\frac{\lambda_i\xi_{im}^{-2}-\lambda_i^{-3}\lambda_j^{-2}\xi_{im}^2\xi_{jm}^2}{1-(\lambda_i^2\xi_{im}^{-2}+\lambda_j^2\xi_{jm}^{-2}+\lambda_i^{-2}\lambda_j^{-2}\xi_{im}^2\xi_{jm}^2-3)/J_m^{\beta}}-\frac{P_i}{\mu^{\alpha}L_jH}-\frac{\varepsilon\phi^2}{\mu^{\alpha}H^2}\lambda_i\lambda_j^2=0 \tag{9}$$

and

$$\left(\frac{c_mL_i}{2L_jH}+\frac{c_mH}{2L_iL_j}\xi_{im}^{-4}\xi_{jm}^{-2}\right)\frac{d\xi_{im}}{dt}+\frac{c_mH}{2L_iL_j}\xi_{im}^{-3}\xi_{jm}^{-3}\frac{d\xi_{jm}}{dt}=\frac{\mu_m^{\beta}(\lambda_i^2\xi_{im}^{-3}-\lambda_i^{-2}\lambda_j^{-2}\xi_{im}\xi_{jm}^2)}{1-(\lambda_i^2\xi_{im}^{-2}+\lambda_j^2\xi_{jm}^{-2}+\lambda_i^{-2}\lambda_j^{-2}\xi_{im}^2\xi_{jm}^2-3)/J_m^{\beta}}. \tag{10}$$

Thereby, the dynamical model of the viscoelastic DEs is preliminarily deduced. As shown in Fig. 3, in order to consider the geometrical effects, we define the length and width of DEs as

$$L_1=N_1H \tag{11}$$

and

$$L_2=N_2H, \tag{12}$$

where N_1 and N_2 are the dimensionless multiples. Under such a condition, the length and width of DE membranes can be random multiples of the thickness. By inserting Eqs. (11) and (12) into the governing equations (9) and (10), the dynamical model of viscoelastic DEs is generalized and obtained as

$$(N_i^2+\lambda_i^{-4}\lambda_j^{-2})\frac{d^2\lambda_i}{dT^2}+\lambda_i^{-3}\lambda_j^{-3}\frac{d^2\lambda_j}{dT^2}-2\lambda_i^{-2}\lambda_j^{-1}\left[\lambda_i^{-3}\lambda_j^{-1}\left(\frac{d\lambda_i}{dT}\right)^2+\lambda_i^{-1}\lambda_j^{-3}\left(\frac{d\lambda_j}{dT}\right)^2+\lambda_i^{-2}\lambda_j^{-2}\frac{d\lambda_i}{dT}\frac{d\lambda_j}{dT}\right]$$
$$+\frac{\lambda_i-\lambda_i^{-3}\lambda_j^{-2}}{1-(\lambda_i^2+\lambda_j^2+\lambda_i^{-2}\lambda_j^{-2}-3)/J^{\alpha}}+\sum_{m=1}^{n}\frac{\mu_m^{\beta}}{\mu^{\alpha}}\frac{\lambda_i\xi_{im}^{-2}-\lambda_i^{-3}\lambda_j^{-2}\xi_{im}^2\xi_{jm}^2}{1-(\lambda_i^2\xi_{im}^{-2}+\lambda_j^2\xi_{jm}^{-2}+\lambda_i^{-2}\lambda_j^{-2}\xi_{im}^2\xi_{jm}^2-3)/J_m^{\beta}}-\frac{1}{N_j}\overline{P_i}-\Phi^2\lambda_i\lambda_j^2=0 \tag{13}$$

and

$$\left(\frac{N_i}{N_j}+\frac{1}{N_iN_j}\xi_{im}^{-4}\xi_{jm}^{-2}\right)\frac{d\xi_{im}}{dT}+\frac{1}{N_iN_j}\xi_{im}^{-3}\xi_{jm}^{-3}\frac{d\xi_{jm}}{dT}=\frac{1}{C_m}\frac{\lambda_i^2\xi_{im}^{-3}-\lambda_i^{-2}\lambda_j^{-2}\xi_{im}\xi_{jm}^2}{1-(\lambda_i^2\xi_{im}^{-2}+\lambda_j^2\xi_{jm}^{-2}+\lambda_i^{-2}\lambda_j^{-2}\xi_{im}^2\xi_{jm}^2-3)/J_m^{\beta}}, \tag{14}$$

in which $T=t/\sqrt{[(\rho H^2)/3\mu^{\alpha}]}$ is the dimensionless time, $\overline{P_i}=[P_i/(\mu^{\alpha}H^2)]$ $(i=1,\ 2)$ is the dimensionless tensile force, $\Phi=(\phi/H)\sqrt{\varepsilon/\mu^{\alpha}}$ is the dimensionless voltage, and $C_m=(c_m/\mu_m^{\beta})[1/(2H^2)]\sqrt{[(3\mu^{\alpha})/\rho]}$ is the dimensionless viscous damping. Hence, the dynamical model for viscoelastic DEs is established. Based on this model, the geometrical effects of DEs on dynamic performances can be explored and predicted. Also, a DE membrane with

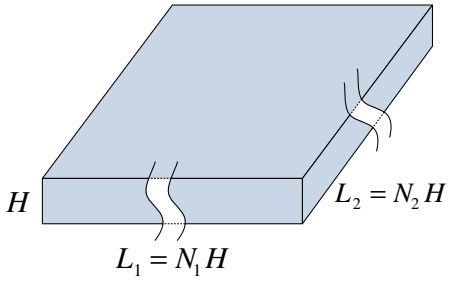

FIG. 3. A schematic to describe the geometrical effects of DEs. The length and width of DEs are related to random multiples of the thickness.

an arbitrary rectangular dimension can be modeled and theoretically described by varying the values of N_1 and N_2. As the Wiechert model consists of n groups of Maxwell units and cannot be completely involved, we only consider three of them in the following calculation. The required material parameters for calculations are set as follows, $\mu^{\alpha}/\mu_m^{\beta} = 1$, $J^{\alpha} = J_m^{\beta} = 100$, $C_1 = 0.1$, $C_2 = 0.01$, $C_3 = 0.001$. The periodic sinusoidal voltage $\Phi = \Phi_0 \sin(\Omega T)$ is applied to stimulate the nonlinear vibration of DEs, in which Φ_0 denotes the dimensionless voltage amplitude, and Ω is the dimensionless voltage frequency. In the following calculation process, the parameters of applied voltage are set as $\Phi_0 = 0.5$ and $\Omega = 0.1$.

III. DYNAMIC PROPERTIES OF DES WITHOUT TENSILE FORCES

Since the tensile forces may affect geometrical boundaries and tune the dynamic properties [22,24,26], therefore, we study the dynamic performances of DEs with and without tensile forces, respectively. In this section, we investigate the dynamic properties of DEs without tensile forces by incorporating the geometrical effects. Both the square and rectangular DE membranes are considered.

A. Square DEs with different geometrical sizes

In this subsection, by combining Eqs. (13) and (14) and setting $\overline{P_1} = \overline{P_2} = 0$, we theoretically detect the dynamic properties of viscoelastic DEs with square sizes. N_1 and N_2 are prescribed as $N_1 = N_2$ in order to guarantee the square DEs. Under such a square case, the dynamic responses of λ_1 and λ_2 are identical to each other, that is, $\lambda_1 = \lambda_2 = \lambda$.

Figure 4 describes the dynamic response of the square viscoelastic DEs when the geometrical sizes are set as $N_1 = N_2 = 10$, 30, 70, and 90, respectively. When $N_1 = N_2 = 10$, the dynamic response of DEs vibrates the most strongly and nonlinearly, and exhibits the phenomenon of "beating," which does not exist when N_1 and N_2 take other values. During the DEs' nonlinear vibration, we regard the maximum level of the difference between the peak and valley value of λ as $\lambda_{P\text{-}V}$. It can be found that both the value of $\lambda_{P\text{-}V}$ and the nonlinearity weaken gradually when N_1 and N_2 are added. Furthermore, the frequency of the dynamic response also gradually decreases when N_1 and N_2 increase. In addition, the decreasing rate of $\lambda_{P\text{-}V}$ and the frequency of dynamic response reduces as N_1 and N_2 enlarge, resulting from the combination of the extended geometrical sizes and the weakened effect of the inertial force in the thickness direction.

Under the same actuation and boundary conditions in Fig. 4, the corresponding phase paths and the Poincaré maps of the square DEs are illustrated in Fig. 5. The phase paths and the Poincaré maps are used to further detect the dynamic properties of the DE systems [23]. If the points in Poincaré maps overlap to one point, the DE system experiences a periodic vibration. Meanwhile, if the points in Poincaré maps form a closed loop, the DE system undergoes a quasiperiodic vibration. On the contrary, if the points in Poincaré maps are disordered, the dynamic system experiences an aperiodic vibration. When $N_1 = N_2 = 10$, the Poincaré map is disordered, indicative of an aperiodic vibration of DEs, as shown in Fig. 5(a). However, with an increase of N_1 and N_2, the Poincaré map becomes ordered and forms the closed loops, such as $N_1 = N_2 = 30$ [Fig. 5(b)], 70 [Fig. 5(c)], and 90 [Fig. 5(d)], which demonstrates that the DEs under these geometrical sizes undergo the quasiperiodic vibration. Therefore, it can be concluded that a transition from aperiodic vibration to quasi

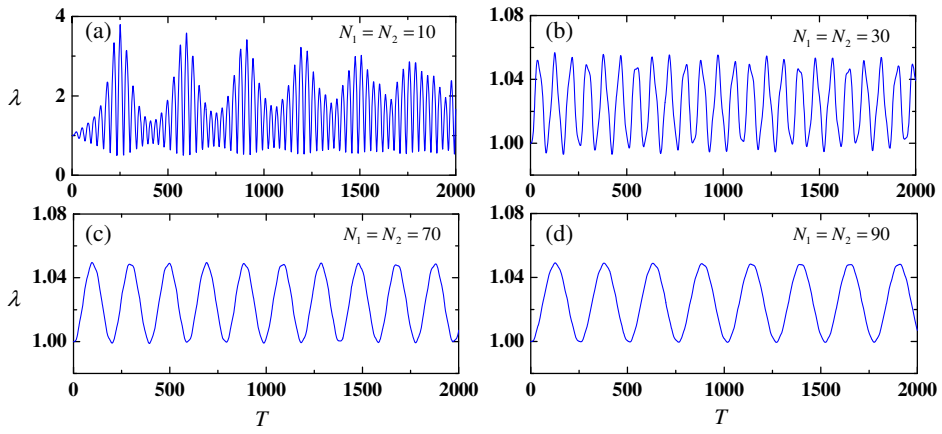

FIG. 4. Dynamic response of square DEs without tensile forces when the geometrical sizes are set as $N_1 = N_2 = 10$, 30, 70, and 90, respectively.

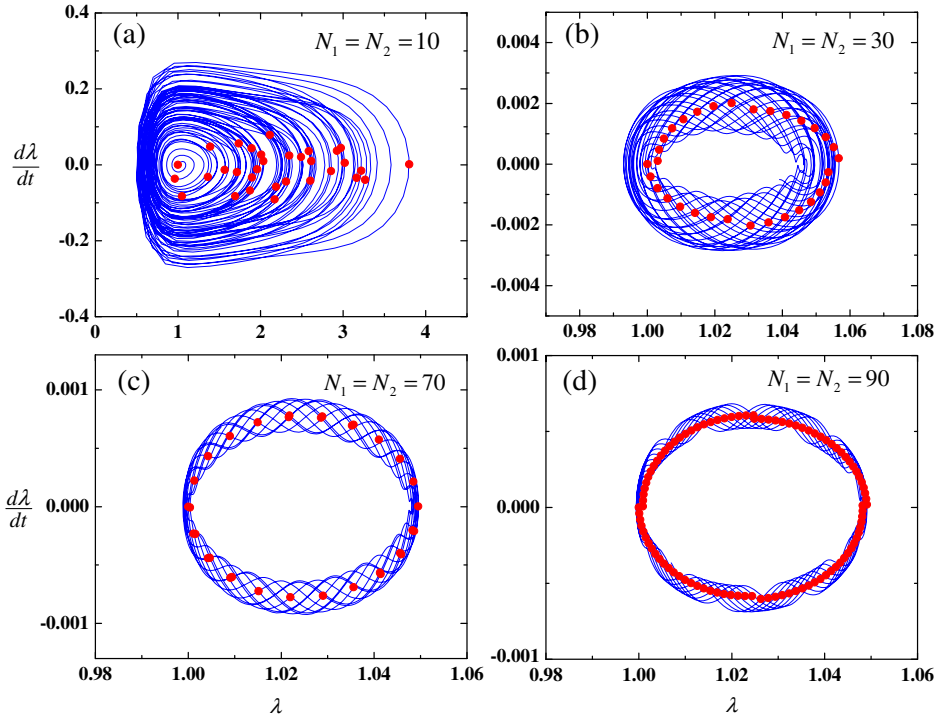

FIG. 5. The phase paths and the Poincaré maps of square DEs without tensile forces when the geometrical sizes are set as $N_1 = N_2 = 10$, 30, 70, and 90, respectively.

periodic vibration of DEs occurs when N_1 and N_2 increase, that is, the increase of areal size of square DEs leads to the DEs transforming from aperiodic vibration to quasiperiodic vibration.

B. Rectangular DEs with different geometrical sizes

Compared with the last subsection, here we investigate the dynamic properties of viscoelastic DEs with rectangular sizes. Also, the tensile forces are prescribed

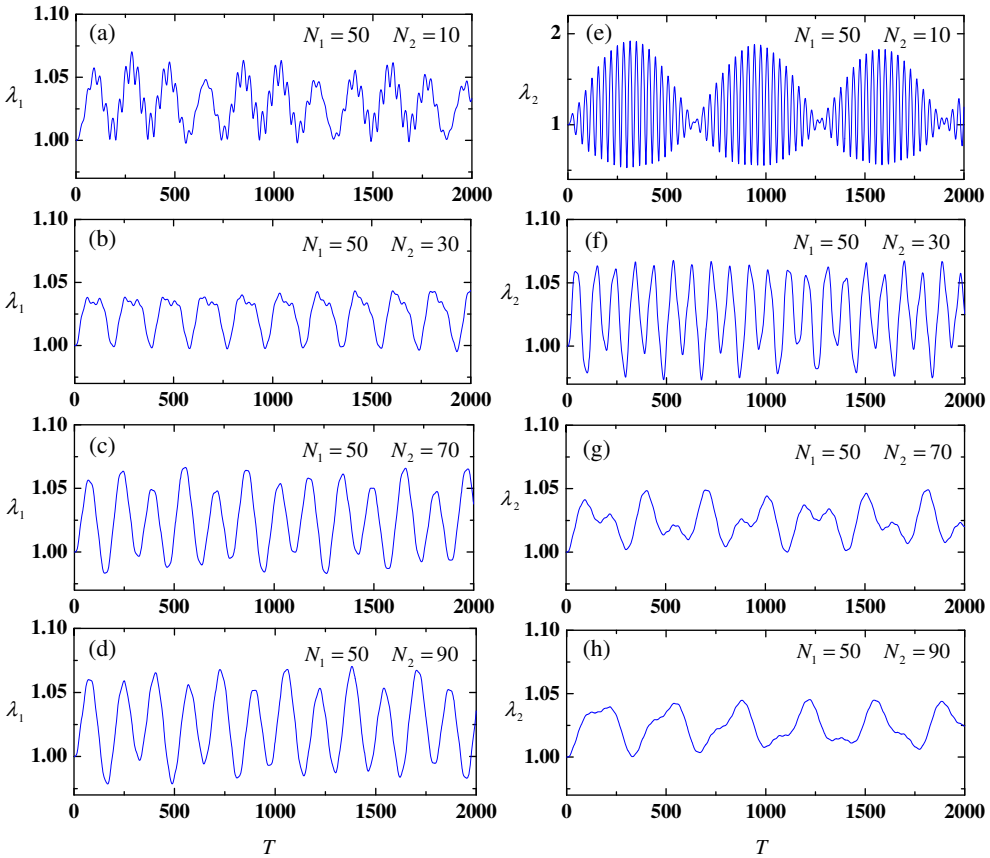

FIG. 6. Dynamic response of rectangular DEs without tensile forces when the geometrical sizes are set as $N_2 = 10$, 30, 70, and 90 with the constant $N_1 = 50$.

as $\overline{P_1} = \overline{P_2} = 0$. In order to obtain the rectangular DE membranes, we set $N_1 = 50$ as a constant and vary the values of N_2 from $N_2 = 10$, 30, 70, to 90. Under such a condition, λ_1 and λ_2 are nonidentical and coupled with each other during the DE's vibration.

The dynamic response of λ_1 and λ_2 of the rectangular DEs is exhibited in Fig. 6 when the tensile forces are set as $\overline{P_1} = \overline{P_2} = 0$. When N_2 is less than N_1, the stretch λ_2 shows a stronger vibration than λ_1, as shown in Figs. 6(a) and 6(b) and Figs. 6(e) and 6(f). Particularly, when $N_1 = 50$ and $N_2 = 10$, λ_2 vibrates the strongest and the beating is induced [Fig. 6(e)]. As N_2 adds up and exceeds N_1, the dynamic response of λ_1 becomes stronger than that of λ_2, as revealed in Figs. 6(c) and 6(d) and Figs. 6(g) and 6(h).

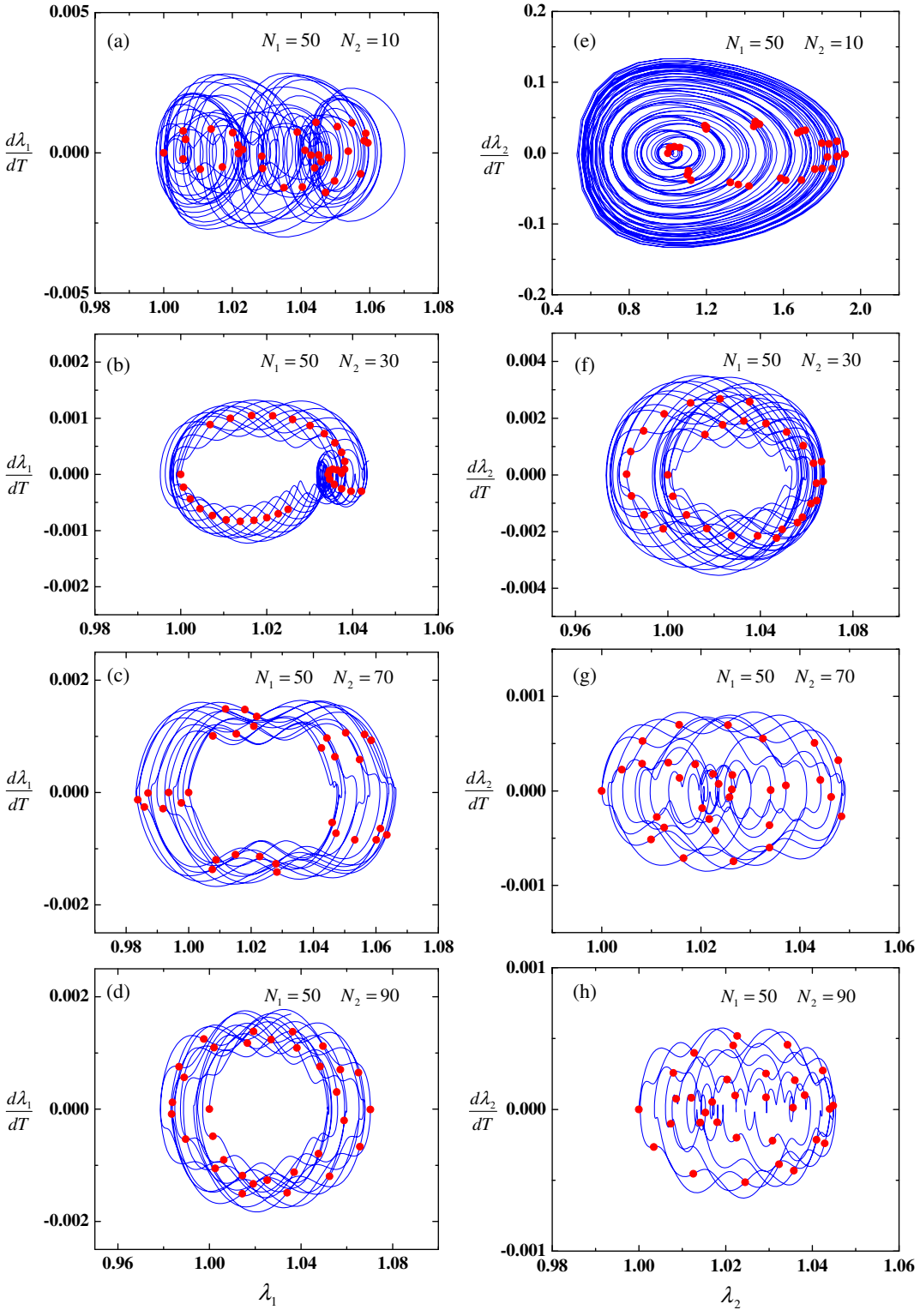

FIG. 7. The phase paths and the Poincaré maps of rectangular DEs without tensile forces when the geometrical sizes are set as $N_2 = 10$, 30, 70, and 90 with the constant $N_1 = 50$.

Furthermore, for the vibration of λ_1, the nonlinearity weakens when the value of N_2 increases. However, an increase of N_2 enhances the nonlinearity in the vibration of λ_2. The above analysis implies that a larger geometrical scale in a certain in-plane direction suppresses the dynamic response and enhances the nonlinearity in this direction.

When the same actuation and boundary conditions are consistent with Fig. 6, the corresponding phase paths and the Poincaré maps of λ_1 and λ_2 of the rectangular DEs are given in Fig. 7. We first consider the case when N_2 is smaller than N_1. When $N_2 = 10$, the Poincaré maps of both λ_1 and λ_2 are quite disordered, as shown in Figs. 7(a) and 7(e). Subsequently, the Poincaré maps of both λ_1 and λ_2 become somewhat ordered and form some bunches when the value of N_2 adds up to 30, which is revealed in Figs. 7(b) and 7(f). After N_2 is beyond the prescribed value of $N_1 = 50$, such as $N_2 = 70$ and 90, the Poincaré maps of both λ_1 and λ_2 go back to the disordered state. According to the results in Fig. 5, the DEs with square geometry may undergo the quasiperiodic vibration. As for the case in Fig. 7, all the Poincaré maps are disordered whenever N_2 is below or beyond the prescribed value of $N_1 = 50$, and the Poincaré maps become somewhat ordered and form some bunches when N_2 is close to 50. Therefore, it can be concluded that, when the geometrical size in a certain in-plane direction increases and the geometrical size in another certain in-plane direction is prescribed as a constant, the DEs experience two transitions: a first transition from aperiodic vibration to quasiperiodic vibration, and a second transition from quasiperiodic vibration to aperiodic vibration.

IV. DYNAMIC PROPERTIES OF DES WITH TENSILE FORCES

In Sec. III, the dynamic properties of DEs without the tensile forces are considered. In this section, we study the dynamic performances of DEs by incorporating the effects of tensile forces and geometrical sizes. In order to focus on the geometrical effects, we apply the equal-biaxial dimensionless tensile forces of $\overline{P_1} = \overline{P_2} = 0.5$. Respectively, we consider the effects of both small and large geometrical sizes on the dynamic properties of rectangular DEs under equal-biaxial tensile forces.

A. Rectangular DEs with small geometrical sizes

In this subsection, by employing the dimensionless tensile forces $\overline{P_1} = \overline{P_2} = 0.5$, we study the dynamic performance of rectangular DEs with relatively small geometrical sizes. The calculation results are described in Fig. 8. We keep $N_1 = 5$ as the constant and vary N_2 between 1 and 10. An increase of N_2 from 1 and 10 leads to a reduction of the mean stretch of λ_1, and induces an enlargement of the mean stretch of λ_2. During the nonlinear vibration, the mean stretch of DEs is defined as half of the sum of the peak and valley value of λ. Furthermore, as N_2 increases from 1 and 10, $\lambda_{P\text{-}V}$ of λ_1 reduces and $\lambda_{P\text{-}V}$ of λ_2 enlarges.

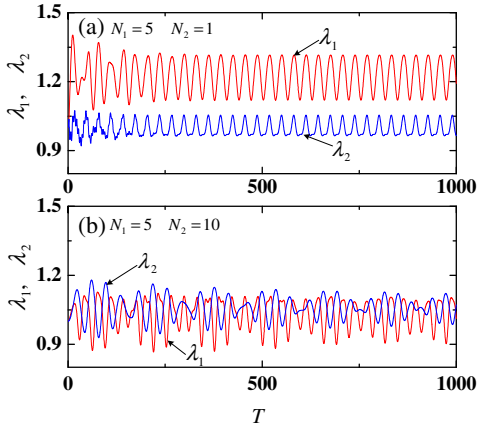

FIG. 8. By employing the equal-biaxial dimensionless tensile forces of $\overline{P_1} = \overline{P_2} = 0.5$, the dynamic response of λ_1 and λ_2 of rectangular DEs with relatively small geometrical sizes. (a) $N_1 = 5$, $N_2 = 1$; (b) $N_1 = 5$, $N_2 = 10$.

Subject to the tensile forces of $\overline{P_1} = \overline{P_2} = 0.5$, the corresponding phase paths and the Poincaré maps of λ_1 and λ_2 of the rectangular DEs with small geometrical sizes are presented in Fig. 9. All the phase paths are disordered and appear as a tangle of interlaced curves, indicating the DEs possess very complicated nonlinear behavior. In addition, all the Poincaré maps are disordered and do not form the closed loops, detecting that the DEs experience the aperiodic vibration.

B. Rectangular DEs with large geometrical sizes

Compared with the last subsection, here we consider the dynamic characteristics of rectangular DEs with relatively large geometrical sizes by applying the identical tensile forces $\overline{P_1} = \overline{P_2} = 0.5$. In the simulation, $N_1 = 50$ is set as the constant, and N_2 is tuned from 10 to 100. Similar to Figs. 8(a) and 8(b), both the mean stretch and $\lambda_{P\text{-}V}$ of λ_1 reduce when N_2 enlarges from 10 to 100. However, for the vibration of λ_2, both the mean stretch and $\lambda_{P\text{-}V}$ also decrease as N_2 increases, which is not consistent with the results in Figs. 8(a) and 8(b).

Under the same actuation conditions in Fig. 10, the corresponding phase paths and the Poincaré maps of λ_1 and λ_2 of the rectangular DEs with large geometrical sizes are presented in Fig. 11. Similar to the results in Fig. 9, the phase paths are all emerging as tangles of interlaced curves, implying a complicated nonlinear vibration. Also, all the Poincaré maps are disordered and do not form the closed loops, demonstrating an aperiodic vibration of DEs. However, when the geometrical sizes of DEs are set as $N_1 = 50$ and $N_2 = 10$, the Poincaré maps of both λ_1 and λ_2 appear as some groups of ordered bunches, declaring that DEs are approaching the quasiperiodic vibration.

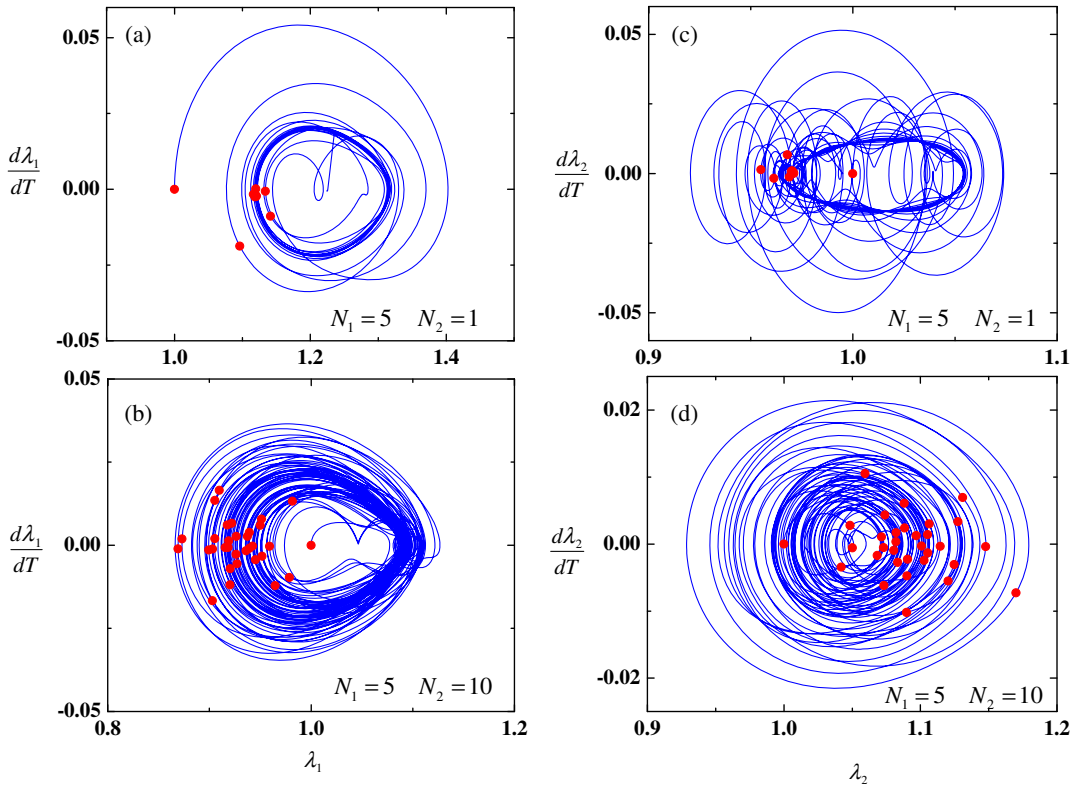

FIG. 9. By employing the equal-biaxial dimensionless tensile forces of $\overline{P_1} = \overline{P_2} = 0.5$, the phase paths and the Poincaré maps of λ_1 and λ_2 of rectangular DEs with relatively small geometrical sizes. $N_1 = 5$, $N_2 = 1$ for (a) λ_1 and (c) λ_2; $N_1 = 5$, $N_2 = 10$ for (b) λ_1 and (d) λ_2.

Combining Figs. 8–11, we conclude that the geometrical sizes largely affect the dynamic performances of DEs that subject to the equal-biaxial tensile forces. When the geometrical sizes of DEs are comparably small, enlargement of the geometrical size in a certain in-plane direction (the geometrical size in another in-plane direction is set as a constant) enhances the vibration in this direction and suppresses the vibration in another in-plane direction. However, when the geometrical sizes of DEs are comparably large, the vibrations in both of the two in-plane directions are suppressed as the geometrical size in a certain in-plane direction increases (the geometrical size in another in-plane direction is set as a constant). Such a conclusion results from the combined effects of the geometrical sizes of DEs and the external tensile forces, leading to the different variation of the mean stretch and $\lambda_{P\text{-}V}$ of DEs with comparably small and large geometrical sizes.

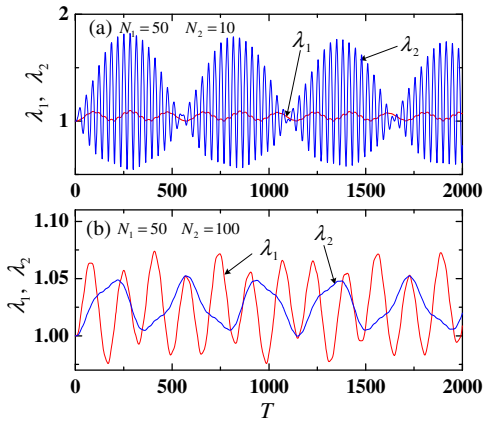

FIG. 10. By employing the equal-biaxial dimensionless tensile forces of $\overline{P_1} = \overline{P_2} = 0.5$, the dynamic response of λ_1 and λ_2 of rectangular DEs with relatively large geometrical sizes. (a) $N_1 = 50$, $N_2 = 10$; (b) $N_1 = 50$, $N_2 = 100$.

V. ANALYSIS OF RESONANCE CHARACTERISTICS

In the above analysis, the dynamic properties of DEs under a specific voltage frequency are investigated. In this section, we explore the effects of geometrical sizes on resonance characteristics of DEs by involving the whole frequency ranges. We assume that when $\lambda_{P\text{-}V}$ peaks, the resonance of DEs occurs. The frequency when $\lambda_{P\text{-}V}$ peaks is regarded as the resonant frequency Ω_R, and the peak value of $\lambda_{P\text{-}V}$ at the resonant frequency Ω_R is defined as $\lambda_{P\text{-}V}(\Omega_R)$. In this section, the $\lambda_{P\text{-}V}$ of λ_1 is considered.

When DEs are with no tensile forces, that is $\overline{P_1} = \overline{P_2} = 0$, the frequency-response spectrums of DEs are exhibited in Fig. 12. Both the square and rectangular DE membranes are considered. Figure 12(a) illustrates the frequency-response spectrums of square DEs. When the geometrical sizes of DEs range from $N_1 = N_2 = 10$ to 90, both Ω_R and $\lambda_{P\text{-}V}(\Omega_R)$ reduce gradually. By keeping $N_1 = 50$ as a constant and varying the value of N_2, the frequency-response spectrums of rectangular DEs are obtained, as

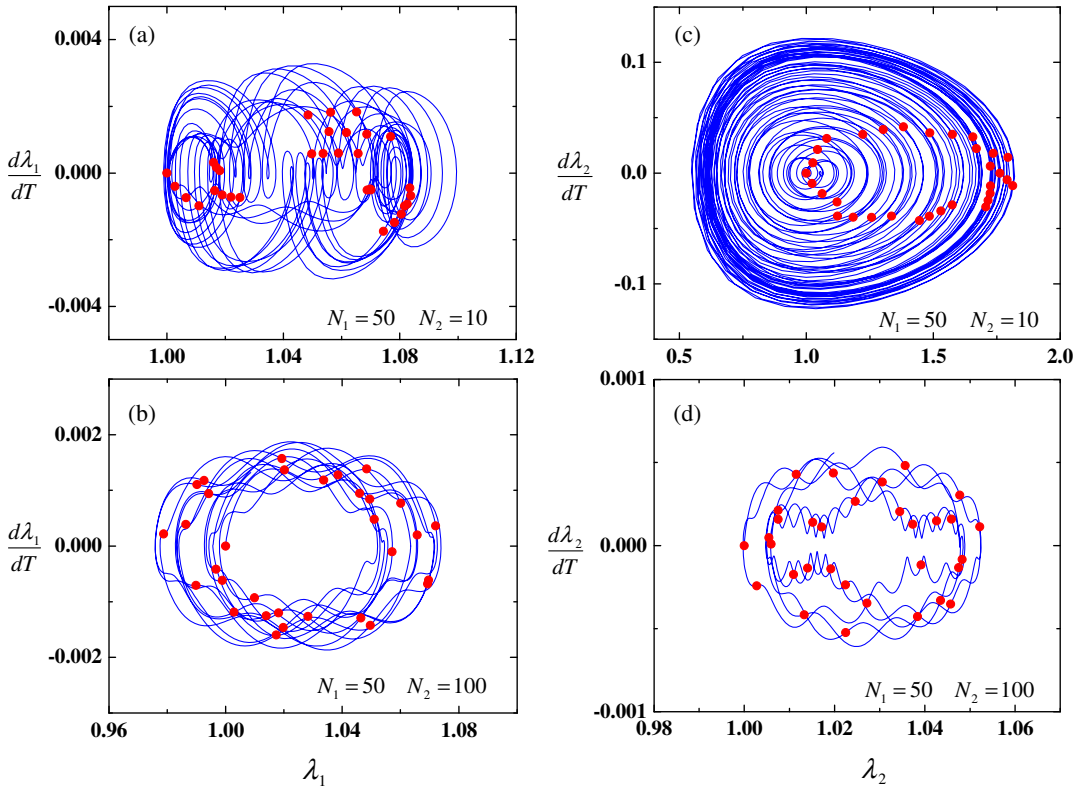

FIG. 11. By employing the equal-biaxial dimensionless tensile forces of $\overline{P_1} = \overline{P_2} = 0.5$, the phase paths and the Poincaré maps of λ_1 and λ_2 of rectangular DEs with relatively large geometrical sizes. $N_1 = 50$, $N_2 = 10$ for (a) λ_1 and (c) λ_2; $N_1 = 50$, $N_2 = 100$ for (b) λ_1 and (d) λ_2.

given in Fig. 12(b). When N_2 is smaller than N_1, the increase of N_2 dramatically causes a reduction of both Ω_R and $\lambda_{P\text{-}V}(\Omega_R)$, such as the increase of N_2 from 10 to 30. On the other hand, when N_2 is larger than N_1, the resonant frequency Ω_R is weakly decreased as N_2 enlarges from 100 to 200. However, the peak value $\lambda_{P\text{-}V}(\Omega_R)$ almost stays invariable and is rarely affected by an increase of N_2. The reason is due to the combination of the augmented in-plane geometrical sizes and the weakened inertial effect in the thickness direction.

Figure 13 provides the frequency-response spectrums of rectangular DEs under the tensile forces $\overline{P_1} = \overline{P_2} = 0.5$. Two kinds of DEs with relatively small and large

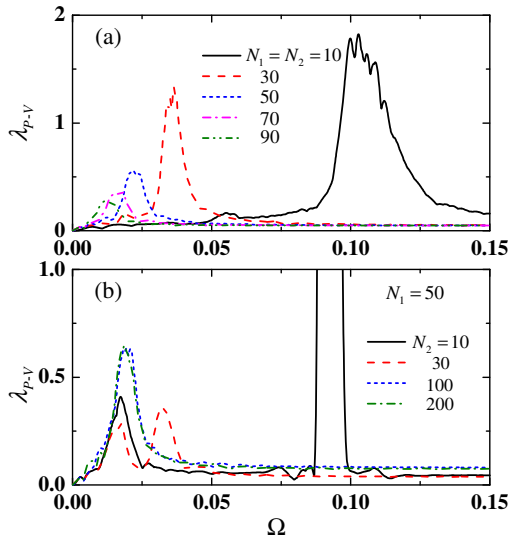

FIG. 12. Under no tensile forces, the frequency-response spectrums of DEs with consideration of geometrical effects. (a) The square DE membranes with different geometrical sizes. (b) The rectangular DE membranes with different geometrical sizes.

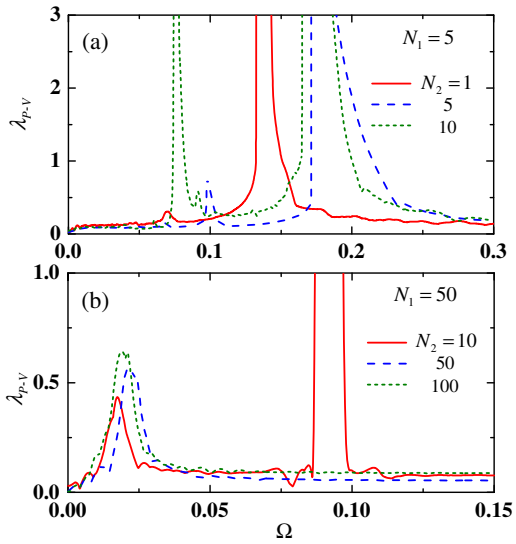

FIG. 13. Under the tensile forces $\overline{P_1} = \overline{P_2} = 0.5$, the frequency-response spectrums of rectangular DEs with consideration of geometrical effects. (a) The DE membranes with different small geometrical sizes. (b) The DE membranes with different large geometrical sizes.

geometrical sizes are investigated. As shown in Fig. 13(a), when $N_1 = 5$ is kept as the constant and N_2 is tuned from 1 to 5 and 10, the geometrical effects on resonance properties of DEs are revealed. The resonant frequency Ω_R initially increases when N_2 enlarges from 1 to 5, and subsequently reduces when N_2 further enlarges from 5 to 10. Besides, the peak values $\lambda_{P\text{-}V}(\Omega_R)$ seem unbounded, implying the electromechanical breakdown occurs. When $N_1 = 50$ is kept and N_2 ranges from 10 to 50 and 100, the geometrical effects on resonance characteristics of DEs are presented in Fig. 13(b). The resonant frequency Ω_R reduces as the value of N_2 increases. Simply, the reductive process can be divided into two stages: the dramatic reduction of Ω_R between $N_2 = 10$ and 50; the weak reduction of Ω_R between $N_2 = 50$ and 100. Similarly, the reason is due to the combination of the augmented in-plane geometrical sizes and the weakened inertial effect in the thickness direction.

Based on the modeling work, the various dynamic performances of DEs with different geometrical sizes are revealed. Under the external stimuli, DEs are the versatile materials for potential applications as soft sensors and actuators. When the ac voltage is applied, the DE-based configurations and structures can work as the dynamic electromechanical actuators, such as pumps, loudspeakers, flying wings, acoustic absorbers, electric fish, etc. As we know, for a vibrational system, including the DE system, the dynamic properties are strongly affected by the geometrical sizes. However, previous modeling work on DE dynamics totally ignored the effects of geometrical sizes of DEs. This research explores the geometrical effects on dynamic performances of DEs by deducing a nonlinear viscoelastic dynamical model. Nowadays, various researchers have designed many kinds of dynamic DE actuators, which own different geometrical sizes, respectively. Therefore, the various DE actuators have different working frequencies, vibrational amplitudes, and vibrational periodicity. People have to carefully select the applied voltage value and frequency to guarantee the stable vibration and avoid the unwelcome dynamic instabilities. In this paper, we consider the geometrical effects of DEs on the nonlinear dynamic properties. Based on the present work, people can clearly select the required voltage value and frequency when they actuate the designed DE actuators. According to the structural need, people first can design the required geometrical sizes of the DE actuators, and then they can select the adequate voltage for actuation to avoid the failure and achieve the stable vibration. On the other hand, according to the functional need, people first can select the required geometrical sizes of DEs, and then design the corresponding actuators that own the desired actuations. From both of these points of view, it can be found that this work can advance the development of DEs as actuators, that is, this work can be utilized to design and fabricate the practical DE actuators.

VI. CONCLUSIONS

In this article, by incorporating the geometrical effects, we develop a dynamic model to investigate the dynamic performances of viscoelastic DEs. The dynamic model enables a prediction of the dynamic properties of DEs with arbitrary rectangular geometrical sizes. In addition, the DEs with and without external tensile forces are involved to explore the dynamic properties, respectively. The main results can be summarized as follows. When DEs are with no tensile forces, the dynamic response of square DEs is suppressed and the response frequency is reduced when the geometrical sizes of DEs increase. Furthermore, the DEs experience a transition from aperiodic vibration to quasiperiodic vibration as the geometrical sizes of DEs increase. For rectangular DEs without tensile forces, the dynamic response is comparably suppressed in a certain in-plane direction when the geometrical size in this in-plane direction is beyond the geometrical size in another in-plane direction. Besides, rectangular geometrical size induces the coupled nonlinear vibration between the two in-plane directions, resulting in an aperiodic vibration of DEs. When DEs are subject to equal-biaxial tensile forces, the dynamic properties of rectangular DEs with small and large geometrical sizes are, respectively, studied. When the geometrical sizes of DEs are comparably small, an enlargement of the geometrical size in a certain in-plane direction enhances the vibration in this direction and suppresses the vibration in another in-plane direction. However, when the geometrical sizes of DEs are comparably large, the vibrations in both of the two in-plane directions are suppressed as the geometrical size in a certain in-plane direction increases. Also, the coupled vibration leads to the aperiodic vibration of rectangular DEs with the equal-biaxial tensile forces. Subsequently, the resonance characteristics of DEs with incorporation of geometrical effects are explored. Without tensile forces, the resonant frequency reduces gradually with the increase of the geometrical sizes of square DEs. For the nonsquare DEs, when the geometrical size in a certain in-plane direction is prescribed, the resonant frequency also reduces with the increase of the geometrical size in another in-plane direction. Subject to the equal-biaxial tensile forces, the resonance properties of rectangular DEs with comparably small and large geometrical sizes are researched. When the geometrical sizes of DEs are comparably small, the enlargement of the geometrical size in a certain in-plane direction induces an initial addition and a subsequent reduction of the resonant frequency. However, when the geometrical sizes of DEs are comparably large, the resonant frequency reduces gradually as the geometrical size in a certain in-plane direction increases. This research reveals the geometrical effects on the dynamic properties of viscoelastic DEs, and provides a dynamics model to describe the DEs with the arbitrary rectangular geometrical sizes. The research results can be used to predict the dynamic performances of

practical DE actuators with random rectangular sizes, and also are helpful to adequately determine the required geometrical sizes of DEs to achieve the desired dynamic properties in practical application.

ACKNOWLEDGMENTS

This work was supported by the China National Postdoctoral Program for Innovative Talents (Grant No. BX201600126), and the China Postdoctoral Science Foundation (Grant No. 2016M600783).

[1] R. Pelrine, R. Kornbluh, Q. Pei, and J. Joseph, High-speed electrically actuated elastomers with strain greater than 100%, Science **287**, 836 (2000).
[2] F. Carpi, S. Bauer, and D. D. Rossi, Stretching dielectric elastomer performance, Science **330**, 1759 (2010).
[3] X. Zhao and Z. Suo, Theory of Dielectric Elastomers Capable of Giant Deformation of Actuation, Phys. Rev. Lett. **104**, 178302 (2010).
[4] N. Cohen and G. deBotton, Electromechanical Interplay in Deformable Dielectric Elastomer Networks, Phys. Rev. Lett. **116**, 208303 (2016).
[5] G. Zurlo, M. Destrade, D. DeTommasi, and G. Puglisi, Catastrophic Thinning of Dielectric Elastomers, Phys. Rev. Lett. **118**, 078001 (2017).
[6] F. Carpi, I. Anderson, S. Bauer, G. Frediani, G. Gallone, M. Gei, C. Graaf, C. Jean-Mistral, W. Kaal, G. Kofod, M. Kollosche, R. Kornbluh, B. Lassen, M. Matysek, S. Michel, S. Nowak, B. O'Brien, Q. Pei, R. Pelrine, B. Rechenbach, S. Rosset, and H. Shea, Standards for dielectric elastomer transducers, Smart Mater. Struct. **24**, 105025 (2015).
[7] C. Keplinger, T. Li, R. Baumgartner, Z. Suo, and S. Bauer, Harnessing snap-through instability in soft dielectrics to achieve giant voltage-triggered deformation, Soft Matter **8**, 285 (2012).
[8] Q. Pei, R. Pelrine, S. Stanford, R. Kornbluh, and M. Rosenthal, Electroelastomer rolls and their application for biomimetic walking robots, Synth. Met. **135–136**, 129 (2003).
[9] D. Tang, C. W. Lim, L. Hong, J. Jiang, and S. K. Lai, Analytical asymptotic approximations for large amplitude nonlinear free vibration of a dielectric elastomer balloon, Nonlinear Dyn. **88**, 2255 (2017).
[10] F. Carpi, G. Frediani, S. Turco, and D. D. Rossi, Bioinspired tunable lens with muscle-like electroactive elastomers, Adv. Funct. Mater. **21**, 4152 (2011).
[11] J. Zhao, J. Niu, D. McCoul, Z. Ren, and Q. Pei, Phenomena of nonlinear oscillation and special resonance of a dielectric elastomer minimum energy structure rotary joint, Appl. Phys. Lett. **106**, 133504 (2015).
[12] T. Li, G. Li, Y. Liang, T. Cheng, J. Dai, X. Yang, B. Liu, Z. Zeng, Z. Huang, Y. Luo, T. Xie, and W. Yang, Fast-moving soft electronic fish, Sci. Adv. **3**, e1602045 (2017).
[13] C. Keplinger, J.-Y. Sun, C. C. Foo, P. Rothemund, G. M. Whitesides, and Z. Suo, Stretchable, transparent, ionic conductors, Science **341**, 984 (2013).
[14] J. Huang, S. Shian, Z. Suo, and D. R. Clarke, Maximizing the energy density of dielectric elastomer generators using equi-biaxial loading, Adv. Funct. Mater. **23**, 5056 (2013).
[15] J. Zhang, B. Li, H. Chen, and Q. Pei, Dissipative performance of dielectric elastomers under various voltage waveforms, Soft Matter **12**, 2348 (2016).
[16] X. Zhao, W. Hong, and Z. Suo, Electromechanical Hysteresis and Coexistent States in Dielectric Elastomers, Phys. Rev. B **76**, 134113 (2007).
[17] J. G. Meier, J. W. Mani, and M. Klüppel, Analysis of carbon black networking in elastomers by dielectric spectroscopy, Phys. Rev. B **75**, 054202 (2007).
[18] X. Zhao and Q. Wang, Harnessing large deformation and instabilities of soft dielectrics: Theory, experiment, and application, Appl. Phys. Rev. **1**, 021304 (2014).
[19] J. Fox and N. Goulbourne, On the dynamic electromechanical loading of dielectric elastomer membranes, J. Mech. Phys. Solids **56**, 2669 (2008).
[20] Z. Lu, M. Shrestha, and G.-K. Lau, Electrically tunable and broader-band sound absorption by using micro-perforated dielectric elastomer actuator, Appl. Phys. Lett. **110**, 182901 (2017).
[21] J. Zhu, S. Cai, and Z. Suo, Resonant behavior of a membrane of a dielectric elastomer, Int. J. Solids Struct. **47**, 3254 (2010).
[22] J. Zhang, H. Chen, B. Li, D. McCoul, and Q. Pei, Coupled nonlinear oscillation and stability evolution of viscoelastic dielectric elastomers, Soft Matter **11**, 7483 (2015).
[23] B.-X. Xu, R. Mueller, A. Theis, M. Klassen, and D. Gross, Dynamic analysis of dielectric elastomer actuators, Appl. Phys. Lett. **100**, 112903 (2012).
[24] J. Zhang, L. Tang, B. Li, Y. Wang, and H. Chen, Modeling of the dynamic characteristic of viscoelastic dielectric elastomer actuators subject to different conditions of mechanical load, J. Appl. Phys. **117**, 084902 (2015).
[25] B. Li, J. Zhang, H. Chen, and D. Li, Voltage-induced pinnacle response in the dynamics of dielectric elastomers, Phys. Rev. E **93**, 052506 (2016).
[26] J. Zhang, H. Chen, and D. Li, Method to Control Dynamic Snap-Through Instability of Dielectric Elastomers, Phys. Rev. Applied **6**, 064012 (2016).
[27] J. Zhang, J Zhao, H. Chen, and D. Li, Dynamic analyses of viscoelastic dielectric elastomers incorporating viscous damping effect, Smart Mater. Struct. **26**, 015010 (2017).
[28] J. Zhou, L. Jiang, and R. E. Khayat, Dynamic analysis of a tunable viscoelastic dielectric elastomer oscillator under external excitation, Smart Mater. Struct. **25**, 025005 (2016).
[29] M. Kollosche, G. Kofod, Z. Suo, and J. Zhu, Temporal evolution and instability in a viscoelastic dielectric elastomer, J. Mech. Phys. Solids **76**, 47 (2015).
[30] H. S. Park and T. D. Nguyen, Viscoelastic effects on electromechanical instabilities in dielectric elastomers, Soft Matter **9**, 1031 (2013).
[31] J. S. Plante and S. Dubowsky, Large-scale failure modes of dielectric elastomer actuators, Int. J. Solids Struct. **43**, 7727 (2006).
[32] L. Liu, H. Chen, J. Sheng, J. Zhang, Y. Wang, and S. Jia, Experimental study on the dynamic response of in-plane deformation of dielectric elastomer under alternating electric load, Smart Mater. Struct. **23**, 025037 (2014).

[33] G.-Y. Gu, U. Gupta, J. Zhu, L.-M. Zhu, and X. Zhu, Modeling of viscoelastic electromechanical behavior in a soft dielectric elastomer actuator, IEEE. Trans. Robot. **33**, 1263 (2017).
[34] Z. Suo, Theory of dielectric elastomers, Acta Mech. Solida Sin. **23**, 549 (2010).
[35] M. Wissler and E. Mazza, Modeling and simulation of dielectric elastomer actuators, Smart Mater. Struct. **14**, 1396 (2005).
[36] C. C. Foo, S. Cai, S. J. A. Koh, S. Bauer, and Z. Suo, Model of dissipative dielectric elastomers, J. Appl. Phys. **111**, 034102 (2012).
[37] W. Hong, Modeling viscoelastic dielectrics, J. Mech. Phys. Solids **59**, 637 (2011).
[38] K. A. Khan, H. Wafai, and T. E. Sayed, A variational constitutive framework for the nonlinear viscoelastic response of a dielectric elastomer, Comput. Mech. **52**, 345 (2013).
[39] J. Zhang, J. Ru, H. Chen, D. Li, and J. Lu, Viscoelastic creep and relaxation of dielectric elastomers characterized by a Kelvin-Voigt-Maxwell model, Appl. Phys. Lett. **110**, 044104 (2017).
[40] H. F. Brinson and L. C. Brinson, *Polymer Engineering Science and Viscoelasticity: An Introduction*, 2nd ed. (Springer, New York, 2008).
[41] M. Hodgins, G. Rizzello, D. Naso, A. York, and S. Seelecke, An electro-mechanically coupled model for the dynamic behavior of a dielectric electro-active polymer actuator, Smart Mater. Struct. **23**, 104006 (2014).
[42] M. N. Silberstein and M. C. Boyce, Constitutive modeling of the rate, temperature, and hydration dependent deformation response of Nafion to monotonic and cyclic loading, J. Power Sources **195**, 5692 (2010).
[43] A. N. Gent, A new constitutive relation for rubber, Rubber Chem. Technol. **69**, 59 (1996).
[44] L. Liu, B. Li, W. Sun, H. Chen, and D. Li, Viscoelastic effect and creep elimination of dielectric elastomers in adversarial resonance, J. Appl. Phys. **120**, 164502 (2016).